JOURNAL OF NEUROTRAUMA 33:652–661 (April 1, 2016)

DOI: 10.1089/neu.2015.4045

Isolated Primary Blast Inhibits Long-Term Potentiation in Organotypic Hippocampal Slice Cultures

Edward W. Vogel III,[1] Gwen B. Effgen,[1] Tapan P. Patel,[2] David F. Meaney,[2] Cameron R. "Dale" Bass,[3] and Barclay Morrison III[1]

Abstract

Over the last 13 years, traumatic brain injury (TBI) has affected over 230,000 U.S. service members through the conflicts in Iraq and Afghanistan, mostly as a result of exposure to blast events. Blast-induced TBI (bTBI) is multi-phasic, with the penetrating and inertia-driven phases having been extensively studied. The effects of primary blast injury, caused by the shockwave interacting with the brain, remain unclear. Earlier *in vivo* studies in mice and rats have reported mixed results for primary blast effects on behavior and memory. Using a previously developed shock tube and *in vitro* sample receiver, we investigated the effect of isolated primary blast on the electrophysiological function of rat organotypic hippocampal slice cultures (OHSC). We found that pure primary blast exposure inhibited long-term potentiation (LTP), the electrophysiological correlate of memory, with a threshold between 9 and 39 kPa·ms impulse. This deficit occurred well below a previously identified threshold for cell death (184 kPa·ms), supporting our previously published finding that primary blast can cause changes in brain function in the absence of cell death. Other functional measures such as spontaneous activity, network synchronization, stimulus-response curves, and paired-pulse ratios (PPRs) were less affected by primary blast exposure, as compared with LTP. This is the first study to identify a tissue-level tolerance threshold for electrophysiological changes in neuronal function to isolated primary blast.

Key words: brain; electrophysiology; *in vitro*; learning; neuron

Introduction

Traumatic brain injury (TBI) has been considered the signature injury of the U.S. military operations in Iraq and Afghanistan for more than a decade.[1] In 2014 alone, there were 24,833 identified cases of TBI within the four branches of the U.S. military, with 83.8% of these cases being mild in severity.[2] The biomechanics of blast-induced injury are complex but classified into four mechanisms: primary blast due to the interaction of the supersonic shockwave with biological tissues; secondary blast due to ejecta causing penetrating injuries; tertiary blast due to blunt impact or rapid acceleration/deceleration leading to injurious deformation within the brain; and quaternary blast due to remaining mechanisms including burning, poisoning, infection, and electromagnetic waves.[3,4] Although the mechanisms and consequences of brain deformation, the mechanism of tertiary injury, are well-studied,[5,6] the existence and pathobiology of TBI due to primary blast injury remain controversial.

Animal studies investigating the effects of primary blast injury have produced conflicting results. Some studies report reduced motor function in the rotarod test following primary blast[7–9]; however, others have reported no decline in motor skills from primary blast.[10–12] Similar discrepancies appear for cognition, as well. Following blast exposure, cognitive performance in the Morris water maze significantly decreased in some studies,[10,13] but not in others.[11,12] These mixed results may be due to the large range of blast-induced TBI (bTBI) models in use today in which many critical factors are not standardized, including injury biomechanics (e.g., the head acceleration during blast exposure is often not measured[14]), thorax protection, scaling of the blast magnitude and duration, and orientation of the subject to the blast wave.[10,11,15,16]

It remains unclear whether isolated primary blast affects neurological function. Our *in vitro* approach allows for the precise control of injury biomechanics and removes the potentially confounding influence of systemic pathophysiology (e.g., lung damage, ischemia, etc.) and brain deformation due to blast-induced head acceleration.[3] The goal of our study was to determine the minimum primary blast exposure to produce a significant deficit in neuronal network function in the absence of cell death, that is, a tissue-level tolerance criterion for functional deficits. We have previously characterized our blast-injury model, which comprises a shock tube and a fluid-filled sample receiver for exposing organotypic hippocampal slice

[1]Department of Biomedical Engineering, Columbia University, New York, New York.
[2]Department of Bioengineering, University of Pennsylvania, Philadelphia, Pennsylvania.
[3]Department of Biomedical Engineering, Duke University, Durham, North Carolina.

cultures (OHSC) to primary blast.[3,16,17] The system converts the in-air shockwave into an in-fluid pressure transient to simulate the blast-induced intracranial pressure wave for interaction with the brain culture.[16] Previously, in-fluid pressure transients to injure cultures have been implemented in *in vitro* TBI models to simulate non-blast loading and to replicate the loading associated with fluid percussion injury. Those loading conditions with much longer rise times (~5 ms) and durations (~20 ms) differed substantially from the loading conditions of the current study.[18,19] Loading conditions employed in the current study were designed specifically to replicate blast-loading with much faster rise-times (~0.2 ms) and shorter durations (~3 ms).We measured changes in electrophysiological function in OHSC with 60-channel microelectrode arrays (MEAs). Although we have previously reported that electrophysiological deficits occur at lower primary blast levels than cell death,[3] a threshold for functional deficits has not been reported. In this study, we report that a shockwave produced subtle changes in neuronal network function. However, long-term potentiation (LTP) was significantly impaired or eliminated following primary blast exposure of 9 and 39 kPa·ms impulse, respectively. Determining a tolerance threshold could be used to increase safety during military training, as well as improve helmet technology to better protect military personnel.

Methods

Organotypic hippocampal slice culture

All animal procedures were approved by the Columbia University Institutional Animal Care and Use Committee (IACUC). OHSC were generated as previously described.[3,20] In brief, P8-10 Sprague-Dawley rat pups were decapitated, and the brains removed. Hippocampii were excised, sectioned into 400 μm thick slices, and separated aseptically in ice-cold Gey's salt solution supplemented with 25 mM D-glucose (Sigma, St. Louis, MO). Slices were plated onto porous Millipore Millicell™ cell culture membranes (Millipore, Billerica, MA) in Neurobasal™ medium supplemented with 2 mM GlutaMAX™, 1X B27 supplement, 10 mM HEPES, and 25 mM D-glucose (Life Technologies, Grand Island, NY). Every 2 to 3 days, half of the medium was replaced with full-serum medium, containing 50% Minimum Essential Medium, 25% Hank's Balanced Salt Solution, 25% heat inactivated horse serum, 2 mM GlutaMAX, 25 mM D-glucose, and 10 mM HEPES (Sigma). Prior to blast injury, cultures were maintained for 10 to 14 days.

Primary blast exposure

Blast injury methods have been previously described in detail.[16,17] In brief, a shockwave was generated with a 76-mm diameter aluminum shock tube with an adjustable-length driver section (25 mm, 50 mm, and 190 mm used for the current studies) pressurized with helium or nitrogen and a 1240-mm long driven section.[16,17] Individual culture wells were sealed inside sterile, 57 μm-thick, low-density polyethylene bags (Whirl-Pak, Fort Atkins, WI) filled with 10 mL of pre-warmed, serum-free culture medium (containing 75% Minimum Essential Medium, 25% Hank's Balanced Salt Solution, 2 mM GlutaMAX, 25 mM D-glucose, and 10 mM HEPES) that had been equilibrated with 5% CO_2/95% O_2 (37°C) before being placed in the fluid-filled blast receiver, maintained at 37°C. These bags were selected because their acoustic impedance matched that of water, thus preventing attenuation of the pressure transient, as previously reported.[17] The culture and the bag were submerged 85 mm into the receiver column, oriented perpendicular to the pressure wave propagation. The receiver was sealed (without air bubbles) with a polydimethylsiloxane (PDMS) sheet and positioned directly at the shock tube exit (5 mm gap).

Piezoresistive pressure transducers (Endevco 8530B-500, San Juan Capistrano, CA) were flush-mounted at the exit of the shock tube and in the fluid-filled blast receiver at the location of the culture and were oriented perpendicular to the direction of propagation to record side-on (incident) pressure. Analog outputs from the transducers were conditioned using amplifiers (gain of 50) and low-pass filters (corner frequency of 40 kHz; Alligator Technologies, CostaMesa, CA). Signals were digitized with an X-series data acquisition card at 125 kHz and LabVIEW™ 2010 (National Instruments, Austin, TX). Peak overpressure, overpressure duration, and impulse were calculated with custom MATLAB (Mathworks, Natick, MA) code.[17]

For injured cultures, the shock tube was then fired; sham cultures were treated identically except the shock tube was not fired. Four blast exposure levels were utilized (Table 1; levels referenced to Effgen and colleagues, 2014[3]), characterized by the peak pressure (kPa), duration (ms), and impulse (kPa·ms) of the in-air shockwave and the in-fluid pressure transient. Blast levels (specific parameters given below in the Results section) simulated real-world exposures and were chosen both below and above the threshold for causing cell death based on previous studies.[3] Following blast- or sham exposure, the culture was immediately removed from the receiver and returned to the incubator in fresh, full-serum medium.

Cell death measurement

Propidium iodide fluorescence was used to measure cell death immediately prior to and 4 days following injury. Previous studies with this injury model have demonstrated that significant cell death does not occur until 4 days post-injury.[3] OHSC were incubated in 2.5 μM propidium iodide (Life Technologies) in serum-free medium for 1 h before imaging. Images were acquired at the indicated time points using an Olympus IX81 microscope (Olympus America, Center Valley, PA) with 568/24 nm (peak/width) excitation and 610/40 nm emission filters. Following imaging, cultures were returned to fresh, full serum medium. Cell death was

Table 1. Blast Exposure Levels Tested in This Study

	In-air			*In-fluid*		
Exposure level	*Pressure (kPa)*	*Duration (ms)*	*Impulse (kPa·ms)*	*Pressure (kPa)*	*Duration (ms)*	*Impulse (kPa·ms)*
Level 1	106 ± 2	0.25 ± 0.01	9 ± 2	134 ± 2	1.50 ± 0.01	89 ± 1
Level 2	93 ± 3	1.40 ± 0.01	39 ± 1	270 ± 15	2.60 ± 0.20	295 ± 56
Level 4	336 ± 8	0.84 ± 0.01	87 ± 2	598 ± 15	1.85 ± 0.30	440 ± 13
Level 9	424 ± 6	2.31 ± 0.03	248 ± 3	1510 ± 91	2.80 ± 0.10	1420 ± 87

Blast exposures were characterized by three different parameters of the shockwave: peak overpressure (kPa), duration (ms), and impulse (kPa·ms). Four different exposure levels (in addition to sham exposure) were utilized as previously reported by Effgen and colleagues (2014).[3] Parameters are reported for the in-air shockwave and the in-fluid pressure transient. These blast pressure histories are similar to those experienced in-theater.[3]

determined for specific OHSC regions (DG, CA1, CA3), as previously described, using MetaMorph (Molecular Devices, Downingtown, PA).[21] In brief, the same threshold for fluorescence was used to analyze all images at both pre- and post-injury time points for a given culture. Cell death was quantified as the percentage area of a specific region exhibiting fluorescence above the threshold. To confirm OHSC viability after blast, a subset of cultures were exposed to the highest blast level (Level 9) and subsequently subjected to an excitotoxic injury (10mM of glutamate for 3 h) 4 days following blast exposure. OHSC were returned to fresh serum-free medium following excitotoxic exposure, and cultures were imaged for cell death 24h later. Cell death was analyzed by analysis of variance (ANOVA), followed by Dunnett *post hoc* tests with statistical significance set at $p<0.05$ (SPSS version 22, IBM, Armonk, NY).

Electrophysiology

Electrophysiological activity within the OHSC was recorded using 60-channel MEAs (8×8 electrode grid without the corners, 30 μm electrode diameter, 200 μm electrode spacing) 4 to 6 days following blast injury (60MEA200/30iR-Ti-gr, Multi-Channel Systems, Reutlingen, Germany). This time point coincided with the observed delay for increased cell death previously measured in this injury model.[3] Before transferring OHSCs to MEAs, the MEAs were plasma cleaned (Harrick Plasma, Ithaca, NY) and coated with 5 μL of 0.01% nitrocellulose (GE Healthcare Life Sciences, Piscataway, NJ) in methanol (Pharmco-AAPER, Brookfield, CT) to adhere the tissue to the electrodes. Individual OHSCs were excised from the Millipore membranes and inverted onto the MEA. A nylon mesh, harp slice grid (ALA Scientific Instruments, Farmingdale, NY) held the OHSC stationary and helped ensure contact with the electrodes. OHSCs were perfused with artificial cerebral spinal fluid (norm-aCSF) containing 125 mM NaCl, 3.5 mM KCl, 26 mM $NaHCO_3$, 1.2 mM KH_2PO_4, 2.4 mM $CaCl_2$, 1.3 mM $MgCl_2$, 10 mM 4-(2-hydroxyethyl)-1-piperazineethanesulfonic acid (HEPES), and 10 mM glucose (pH = 7.40), which was bubbled with 5% CO_2/95% O_2 and warmed to 37°C, as previously described.[22] Recordings were acquired with an MEA1060-BC amplifier and data acquisition system (Multi-Channel Systems). The system recorded neural signals at 20 kHz with a 6 kHz analog, anti-aliasing filter. Recordings were further filtered in MATLAB using an eighth-order, digital, low-pass (1000 Hz) and a fourth-order, digital, high-pass (0.2 Hz) Butterworth filter. The sample numbers for each injury group for a given recording protocol are listed in the Results section.

Spontaneous activity

Spontaneous neural activity was measured by recording continuously for 3 min from all electrodes within the hippocampus. The raw data were passed through a 60 Hz comb filter using a custom MATLAB script, before neural event activity was detected based on the multi-resolution Teager energy operator.[23–27] Events were characterized by their start time, magnitude, and duration.

Spontaneous network synchronization was also quantified using previously published methods.[26,28–30] Correlation, c^τ, between neural events was calculated for each electrode pair (x and y) given neural event-timing t_i^x and t_j^y ($i=1,\ldots,m_x$; $j=1,\ldots,m_y$) according to[28]:

$$c^\tau(x|y)=\sum_{i=1}^{m_x}\sum_{j=1}^{m_y}J_{ij}^\tau\begin{cases}J_{ij}^\tau=1 \;\; if \;\; 0<t_i^x-t_j^y\le\tau\\ J_{ij}^\tau=\frac{1}{2} \;\; if \;\; t_i^x=t_j^y\\ J_{ij}^\tau=0 \;\; otherwise\end{cases} \quad (1)$$

in which τ was the duration in which two events were considered synchronous (1.5 ms) and m_x&m_y were the total number of events to be compared on each electrode.

Anactivity correlation matrix, Q_{xy}, was calculated as:

$$Q_{xy}=\frac{c^\tau(x|y)+c^\tau(y|x)}{\sqrt{m_x m_y}} \quad (2)$$

with individual entries ranging from 0 (completely uncorrelated) to 1 (perfectly correlated). The eigenvalues, λ_b, and associated eigenvectors, v_{ab}, of the correlation matrix provided insight to the structure of the neuronal activity. To identify clusters of simultaneously active electrodes, the participation index (PI) was calculated for each electrode a that contributed to a cluster b as:

$$PI_{ab}=\lambda_b v_{ab}^2 \quad (3)$$

where v_{ab} represented the a^{th} element of eigenvector b. Electrodes contributing to cluster b were those with $PI\ge0.01$.[29]

To determine statistical significance, randomized surrogate time-series data without correlated activity were generated with an event-rate equal to the measured event-rate of the experimental recordings.[29] The surrogate process was repeated 50 times, and the mean ($\bar{\lambda}_k$) and standard deviation (SD_k) of surrogate eigenvalues were calculated ($k=1,\ldots,M$, where M represented the number of electrodes in the experiment). We identified the number of synchronized clusters that were significantly different from the randomized, asynchronous surrogate clusters as:

$$Number\ of\ Clusters=\sum_k sgn[\lambda_k > (\bar{\lambda}_k'+K\times SD_k)] \quad (4)$$

where sgn was the sign function, λ_k was the eigenvalue of each electrode of the experimental data, and K was a constant ($K=3$ was chosen to provide a 99% confidence level, i.e., $p<0.01$).

Finally, a global synchronization index (GSI), ranging from 0 (random, uncorrelated activity) to 1 (perfectly synchronous, correlated activity on all electrodes), was calculated for the cluster with the highest degree of synchronization:

$$GSI=\begin{cases}\frac{\lambda_M-\bar{\lambda}'}{M-\bar{\lambda}'} \;\; if \;\; \lambda_M > \bar{\lambda}'\\ 0 \;\; otherwise\end{cases} \quad (5)$$

where $\bar{\lambda}'$ was the mean of the largest surrogate eigenvalues, λ_M was the maximal eigenvalue of the correlation matrix from the experimental data, and M was the number of electrodes in the experiment. Active regional percentage in the most synchronized cluster (i.e., the cluster corresponding to λ_M) was quantified as the ratio of regional electrodes involved in the cluster to the total number of electrodes in the respective region.

Spontaneous and synchronization parameters were averaged for a given recording and analyzed by ANOVA, followed by Dunnett *post hoc* tests with statistical significance set as $p<0.05$ (SPSS version 22, IBM). In addition, principal component analysis (PCA) was performed with the built-in MATLAB function *pca.m* on the parameters together to identify significant changes (ANOVA) in the first principal component score (PC1), followed by Dunnett *post hoc* tests. Observed power was calculated for the effect of injury severity (impulse) with $\alpha=0.05$.

Stimulus-response curves

Stimulus-response (SR) curves were generated by applying a constant current, biphasic, bi-polar stimulus (100 μs positive phase followed by 100 μs negative phase) of increasing magnitude (0–200 μA in 10 μA increments) to electrodes located in either the Schaffer collateral (SC) or mossy fiber (MF) pathways, and the data were analyzed with respect to stimulation site. Evoked responses were recorded from each electrode throughout the hippocampal

tri-synaptic circuit. As in previous studies, each electrode's response was fit to a sigmoidal curve[22] as:

$$R(S) = \frac{R_{max}}{1 + e^{m(I_{50} - s)}} \quad (6)$$

R_{max} represented the maximum amplitude of the evoked response and I_{50} represented the current necessary to generate a half-maximal response. The term *m*, which is proportional to the slope of the sigmoidal fit, represented the spread in the firing threshold for the population of neurons.[22,25,27] Data from each electrode were segregated by anatomical region of interest (ROI: CA1, CA3, DG). Each parameter (I_{50}, m, R_{max}) for an electrode was averaged within a region to determine that regional response for any given slice. Data reported for each region are the average across slices within a given experimental group.

A PCA was also performed to identify significant multivariate changes in the SR parameters. Individual parameters as well as PC1were analyzed by ANOVA followed by Dunnett *post hoc* tests with statistical significance set as $p < 0.05$ (SPSS version 22, IBM). Observed power was calculated for the effect of impulse with $\alpha = 0.05$.

Paired-pulse ratios

Short-term plasticity was investigated by delivering two successive stimuli of the same intensity (I_{50}) at interstimulus intervals (ISI) of 20, 35, 50, 70, 100, 140, 200, 300, 500, 1000, and 2000 ms. Paired-pulse ratios (PPR) were calculated as the ratio of the peak-to-peak amplitude of the second response to the peak-to-peak amplitude of the first response. A PPR >1 indicated paired-pulse facilitation (PPF), whereas a PPR <1 indicated paired-pulse depression.[31] ISIs were assigned to one of four bins that are biologically relevant to short-term synaptic plasticity. Short-term ISI (20 ms) produce paired-pulse depression thought to be mediated by the neurotransmitter γ-aminobutyric acid (GABA), specifically via the $GABA_A$ class of GABA receptors.[32,33] Early-mid ISIs (35–100 ms) elicit a rebound in excitation thought to be caused by $GABA_A$ mediated disinhibition and activation of *N*-methyl-D-aspartate (NMDA) receptors.[32,34] Late-mid ISIs (140–500 ms) produce late-phase paired-pulse depression thought to be mediated by $GABA_B$ receptors.[32,35] Lastly, long-term ISIs (>500 ms) are not expected to elicit a response resulting from the interaction of the paired pulse stimulation and instead results in two independent and equal responses.[36,37] PPRs for each bin were averaged across a given recording and analyzed by ANOVA, followed by Dunnett *post hoc* tests with statistical significance set at $p < 0.05$ (SPSS version 22, IBM). Additionally, PC1 was analyzed to identify significant multivariate changes in PPR. Observed power was calculated for the effect of impulse with $\alpha = 0.05$.

Long-term potentiation

In a separate cohort of cultures, the ability to induce LTP was quantified after blast. Baseline behavior was evoked by stimulating at I_{50} once every min for 30 min. LTP was then induced by stimulating across the SC pathway with a high frequency stimulus, which consisted of three trains of 100 Hz pulses applied for 1 sec at I_{50}, with each train separated by 10 sec.[38,39] Immediately following LTP induction, post-LTP responses were evoked by stimulating at I_{50} once every minute for 60 min. LTP induction was calculated as percent potentiation above baseline based on the last 10 min of recording in each recording window. To ensure only stable responses were included for analysis, electrodes were discounted if the coefficient of variance (pre- or post-induction) was greater than 20%.[40] LTP induction was averaged among electrodes within the CA1 and analyzed by ANOVA followed by Dunnett *post hoc* tests with statistical significance set as $p < 0.05$ (SPSS version 22, IBM).

Results

Primary blast induced cell death in the hippocampus was minimal

We observed a region-specific threshold for blast-induced cell death, but the relative amount of cell death was significantly less than excitotoxic insult. Four days following sham injury or blast exposure and prior to electrophysiology recording, cell death was evaluated within the OHSC (Table 1). In all three regions, cell death (Fig. 1) was minimal, but it significantly increased following a Level 9 blast exposure, as compared with sham. Level 4 blast exposure induced minimal, but significant cell death in only the DG but not the CA3 or CA1. Cell death was not significantly increased after Level 2 or Level 1 blast exposure. Although Level 9 blast exposure induced significant cell death in all ROI, it remained

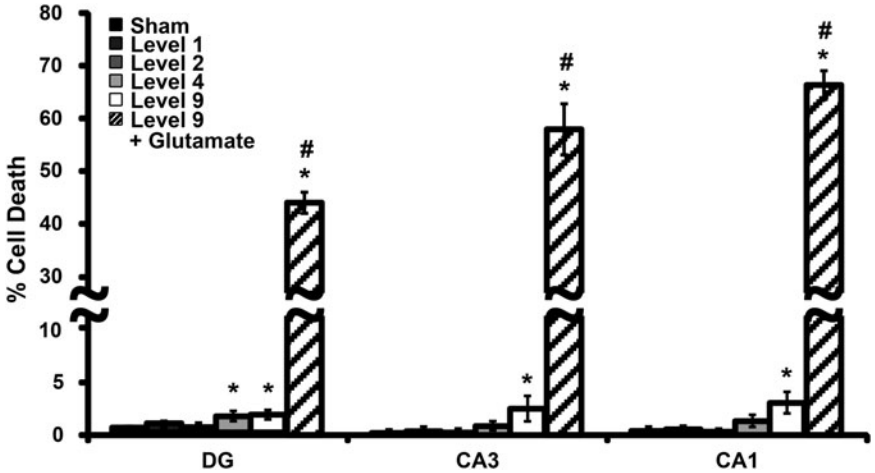

FIG. 1. Cell death measured for each ROI of the hippocampus 4 days after injury. Groups are in order of increasing impulse from left to right. Minimal cell death was significantly induced after Level 9 blast exposure in all ROI. Minimal cell death was significantly induced after Level 4 blast exposure in DG only. Level 2 and Level 1 blast exposure did not significantly increase cell death. Glutamate exposure4 days following Level 9 blast induced significant cell death in all ROI. Mean ± SEM; $n \geq 7$; $^*p < 0.05$ as compared with sham, $^{\#}p < 0.05$ as compared with Level 9. ROI, region of interest; SEM, standard error of mean.

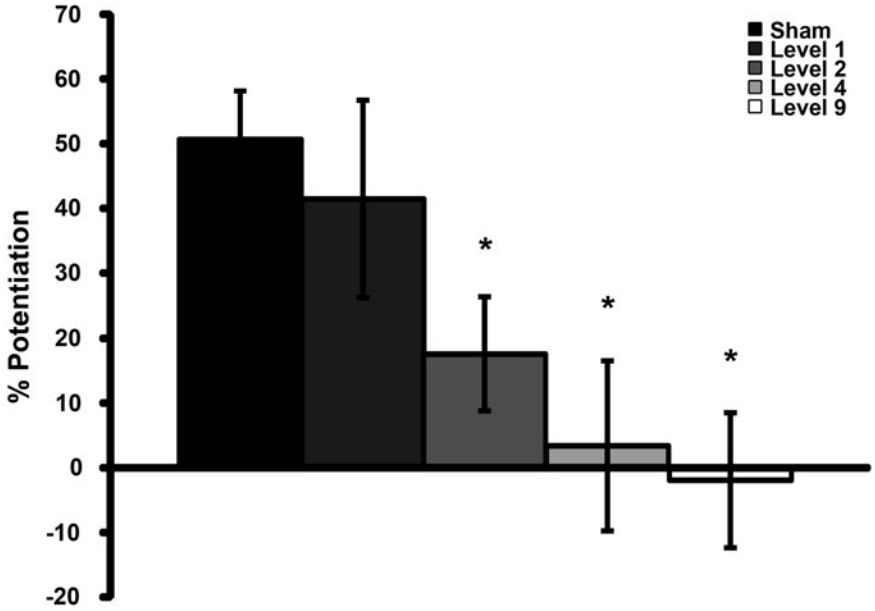

FIG. 2. LTP measured in CA1 4 to 6 days after injury. Groups are in order of increasing impulse from left to right. LTP was significantly reduced after Level 2 and eliminated after Level 4 or Level 9 blast exposures. Mean ± SEM; $n \geq 5$; $^*p < 0.05$, as compared with sham. LTP, long-term potentiation; SEM, standard error of mean.

minimal (<5%). In comparison, glutamate exposure4 days after Level 9 blast exposure significantly increased cell death in all ROIs as compared with a Level 9 blast exposure alone. These data are consistent with a previous study from our group that reported significant but minimal cell death after a Level 9 exposure.[3]

Primary blast exposure impaired long-term potentiation

Four to six days following blast exposure, LTP (Fig. 2) was significantly reduced following Level 9, Level 4, and Level 2 blast exposures as compared with sham. Following Level 1 blast exposure, potentiation closely resembled that of sham-injured cultures.

Primary blast exposure reduced hippocampal synchronization

One feature that is often critical for transmitting information through neural circuitry is the synchronization of activity across distinct regions, an aspect that may underlie the process of memory consolidation.[41] To this end, GSI (Fig. 3A) across recording regions was significantly reduced following Level 9 and Level 4 blast exposures as compared with sham. Blast did not alter the number of synchronized clusters identified (Fig. 3B). Level 9 and Level 4 blast exposure significantly reduced the active regional percentage in the most synchronized cluster (Fig. 3C) in CA3, as compared with sham.

Primary blast exposure minimally affected spontaneous activity

An additional measure to reflect the general excitability of the circuitry is the spontaneous activity recorded within different regions. There was a decreasing trend in spontaneous event rate (Fig. 4A) as the impulse increased from Level 1 to 9 primary blast exposures for all three ROIs; however, the deficits did not reach significance. Level 9 blast exposure significantly decreased spontaneous event magnitude (Fig. 4B) in DG. There was no significant change in event duration (Fig. 4C) after blast exposure for any ROI. Lastly, Level 9 blast exposure significantly reduced PC1 (Fig. 4D) in DG, but the change did not reach statistical significance in CA3 or CA1. PC1 captured more than 95% of the variance in the overall data set. The statistical power was ≥0.18 for all non-significant comparisons.

Primary blast exposure minimally altered basal evoked responses

Spontaneous activity only reveals the state of the circuitry with existing inputs. Alternatively, a full stimulus/response characterization in response to external stimulation would reveal any alterations in the ability to stimulate local circuitry in the OHSC or the progressive stimulation of downstream circuits due to synaptic transmission. When stimulating across the MF pathway, there was no effect on R_{max} (Fig. 5A) or I_{50} (Fig. 5B) following blast exposure, as compared with sham. Level 4 blast exposure significantly decreased the slope of excitation (m) (Fig. 5C) for DG and CA3, as compared with sham. There was no significant change in PC1 (Fig. 5D) for any ROI following blast exposure. PC1 captured more than 99% of the variance in the overall data set. The statistical power was ≥0.20 for all non-significant comparisons.

For stimulation across the SC pathway, Level 9 blast exposure significantly reduced R_{max} (Fig. 6A) in DG, as compared with sham. Level 9 blast exposure significantly increased I_{50} (Fig. 6B) in CA3. Level 9 and Level 4 blast exposure reduced the parameter m (Fig. 6C) in all ROI; however, no change reached significance. Level 9 blast significantly reduced PC1 (Fig. 6D) in DG, as compared with sham. The statistical power was ≥0.31 for all non-significant comparisons.

One explanation for changes in circuit activation would be impairments in presynaptic release, as identified by paired-pulse stimulation paradigms. For stimulation across the MF or SC pathway, primary blast exposure did not change paired-pulse responses (data not shown) in any ROI for any temporal bin of ISIs.

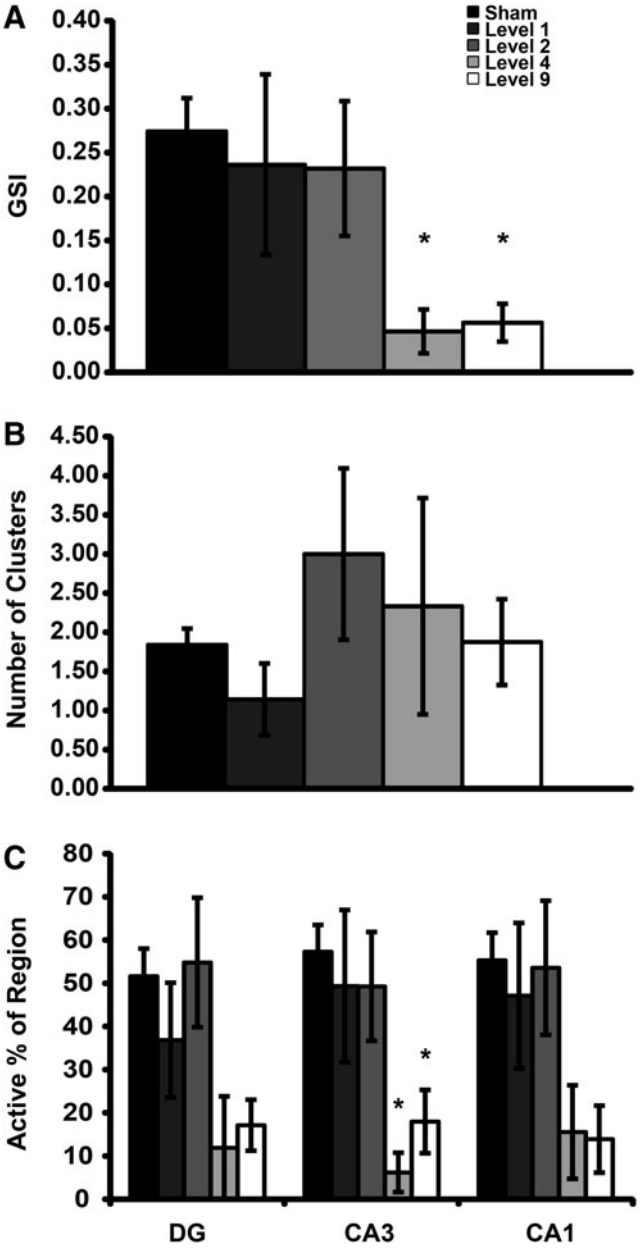

FIG. 3. Synchronization of spontaneous activity 4 to 6 days after injury. Groups are in order of increasing impulse from left to right. The global synchronization index (GSI, [**A**]) was significantly decreased following Level 9 and Level 4 blast exposures compared with sham exposure. The number of synchronized clusters (**B**) per slice was not significantly affected by primary blast exposure ($p \geq 0.43$ with a calculated power of 0.29). Following Level 9 and Level 4 blast exposure, active regional percentage in the most synchronized cluster (**C**) significantly decreased in CA3, as compared with sham exposure. Mean ± SEM; $n \geq 6$; $^*p < 0.05$, as compared with sham. SEM, standard error of mean.

Discussion

The current study reports that 1) primary blast exposure in isolation can disrupt LTP; 2) a threshold for significantly impairing LTP lies between 9 kPa·ms (Level 1) and 39 kPa·ms (Level 2) impulse; 3) primary blast exposure significantly reduced hippocampal synchrony with a threshold lying between 39 kPa·ms (Level 2) and 87 kPa·ms (Level 4) suggesting that synchrony is less sensitive to blast than LTP; and 4) other measures of spontaneous and evoked activity were less sensitive to blast. These functional alterations occurred in the absence of cell death, demonstrating that cell death is not necessary for a change in neuronal function. Functional[42] and cognitive[43] deficits in the absence of cell death have been observed with earlier non-blast models of TBI, as well. Although the highest blast level tested (248 kPa·ms; Level 9) altered electrophysiological function as well as caused significant cell death, average cell death was never above 5% in any ROI, which agreed with previous literature.[3] In comparison, glutamate exposure 4 days following Level 9 blast exposure caused more than 40% cell death in all ROI, confirming the presence of viable cells following blast, which were not injured by primary blast alone.

Although not investigated in previous *in vitro* blast models, LTP has been investigated in acute hippocampal slices following *in vivo* blast exposure. LTP, induced either chemically or by theta-burst stimulation in acute mouse hippocampal slices was significantly reduced 2 and 4 weeks post-blast injury *in vivo* (167 kPa·ms).[11] In this previous work, the injury was a combination of the blast pressure wave through the brain and induced head-acceleration. In general, head acceleration (tertiary blast loading) is a well-known causal factor for brain injury, and therefore it is not possible to prove conclusively that blast pressure alone can cause circuit impairment. Although mild fluid pressure loading to the brain can also cause LTP impairments 1 day,[44] 1 week,[45,46] and 8 weeks[47] post-injury, this injury model is also a mix of pressure and deformation throughout the brain.[48,49] To our knowledge, our data are the first to show that primary blast (shockwave alone) is also capable of disrupting LTP.

Alterations in the function of the hippocampal circuitry after blast was not restricted to only LTP impairments. We found that primary blast exposure reduced global synchronization of hippocampal activity, correlating to observations in humans and other experimental models (Fig. 2A). For example, electroencephalographic synchronization was significantly reduced in the frontal brain regions of U.S. personnel 1 month after blast-exposure without impact.[50] Likewise, non-blast TBI reduced cortical synchronization during learning and recognition tasks.[51] Network synchronization was decreased after *in vitro* stretch injury in both hippocampal slices[26] and cultured cortical neurons.[30] Proposed mechanisms behind these deficits include intracellular chloride imbalance,[26] calpain activation,[30] and loss of white matter tract structural integrity.[50] TBI-induced deficits in network synchronization could explain some short-term learning and memory impairments as previous studies have shown that the basis for working memory is persistent, synchronized neural activity.[52,53] Although previous studies have demonstrated the potential for reduced neural synchrony after various types of injury, our study supports that primary blast exposure, in isolation, is capable of causing deficits in synchronization.

Although spontaneous function (event rate, magnitude, duration) has not been previously investigated after blast injury, the non-blast TBI literature is divided. In our study, our highest blast level (Level 9) was capable of subtly reducing event rate, magnitude, and duration in certain regions of the hippocampus. The decreasing trend for PC1 suggested that clustering the three spontaneous parameters uncovered an underlying deficit in the spontaneous signaling that was not obvious by observing just a single parameter in isolation. After mild controlled cortical impact (CCI) injury in rats, spontaneous event rate was increased in CA1, but not CA3, starting 2 h and out to 24 h post-injury.[54] Alternatively, severe *in vitro* stretch injury decreased spontaneous event rate[55]; however, mild stretch injury did not alter spontaneous event rate at 24 h after injury.[26] These

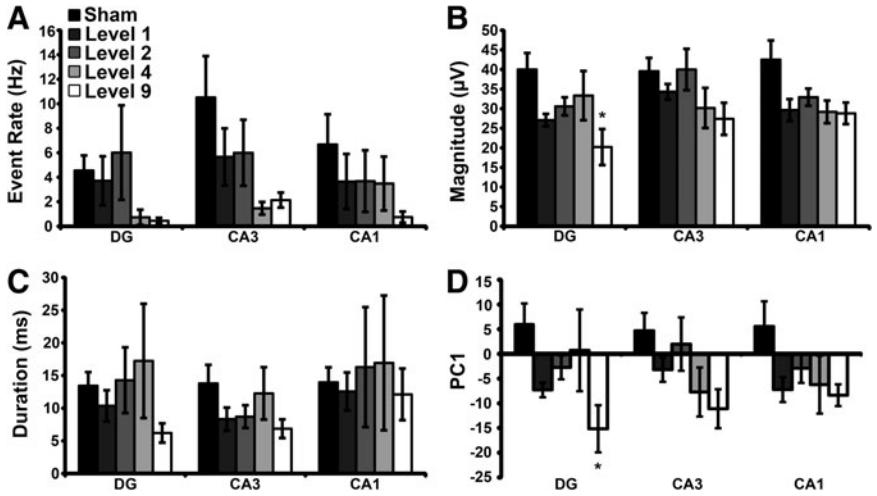

FIG. 4. Blast injury altered spontaneous event properties. There was a decreasing trend in spontaneous event rate (**A**) as impulse increased. Level 9 blast exposure significantly decreased event magnitude (**B**) in DG, as compared with sham. There was no significant change in event duration (**C**) after blast exposure for any ROI ($p > 0.40$ with a calculated power <0.28). Level 9 blast exposure significantly altered PC1 (**D**) in DG, but there was no significant change in CA3 ($p > 0.08$ with a calculated power of 0.54) or CA1 ($p > 0.35$ with a calculated power of 0.33). Mean ± SEM; $n \geq 7$, $^*p < 0.05$, as compared with sham. ROI, region of interest; SEM, standard error of mean.

discrepancies may be related to injury severity and the associated cell death in that spontaneous rates did not change in the absence of cell death.[26] The injury biomechanics between our blast model, the CCI model, and the stretch injury model may contribute to the varying changes following injury. It is possible that the deficits in post-injury synchronization observed in our study could be linked to the slight alterations in the spontaneous functional behavior, but this will need further testing to confirm.

In our study, stimulus-response curves (i.e., input/output curves) were only minimally affected by primary blast exposure, with the largest effects due to a Level 9 blast capable of causing (minimal) cell death. In an *in vivo* rat study, no changes in corpus callosum compound action potentials were measured 3 days post-blast despite cell death in the corpus callosum.[56] However, the duration of the blast was only 200 μs, which is not operationally realistic unless scaled. Applying previously published scaling relationships,[57] this duration would scale to about 2 ms. Non-blast fluid percussion injury increased I_{50} out to 7 days post-injury in rodent CA1[44,58] and decreased R_{max} out to 2 days post-injury in rat CA1[44], in response to SC stimulation. However, similar injury studies reported decreased I_{50}[59] and increased R_{max}[60] between 3 and 7 days post-injury in rodent CA1 in response to SC stimulation. Results from *in vitro*

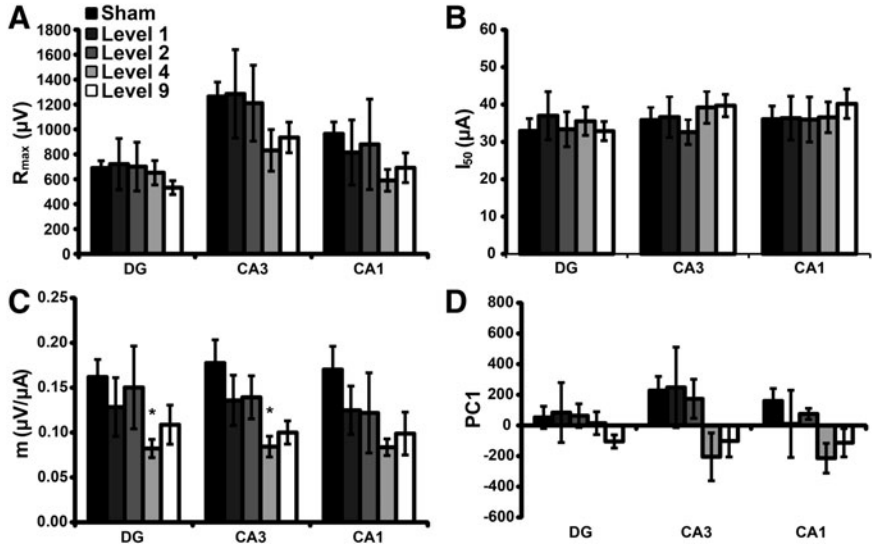

FIG. 5. Blast injury minimally affected stimulus-response parameters when stimulated across the mossy fiber (MF) pathway. There was no significant effect on R_{max} (**A**, $p > 0.14$ with a calculated power <0.12) or I_{50} (**B**, $p > 0.88$ with a calculated power <0.44) following blast exposure, as compared with sham. Level 4 blast exposure significantly reduced m (**C**) in DG and CA3; however, the change did not reach significance in CA1 ($p > 0.09$ with a calculated power of 0.53), as compared with sham exposure. Level 9 exposure reduced m for all ROI, but the changes did not reach significance ($p > 0.07$). There was no significant change ($p > 0.15$ with a calculated power <0.44) in PC1 (**D**) following blast exposure for any ROI. Mean ± SEM; $n \geq 6$, $^*p < 0.05$, as compared with sham. ROI, region of interest; SEM, standard error of mean.

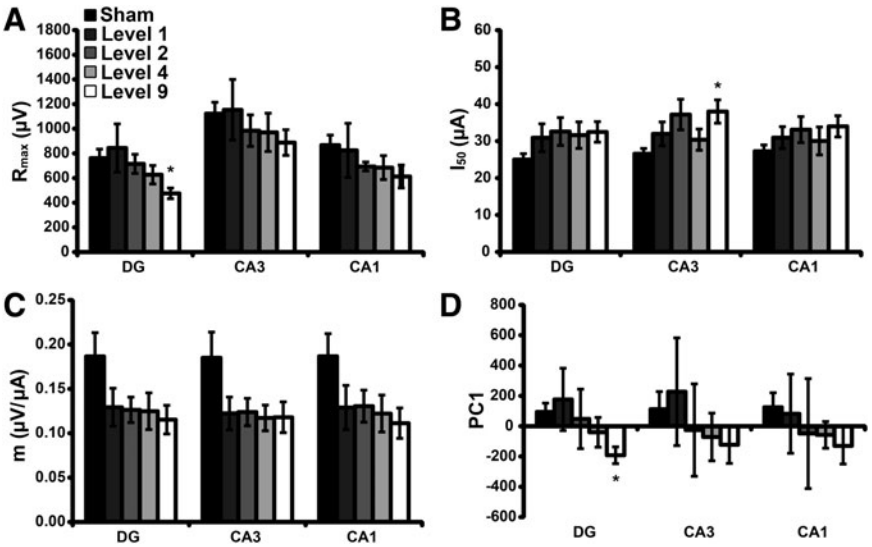

FIG. 6. Blast injury minimally affected stimulus-response parameters when stimulated across the Schaffer collateral (SC) pathway. Level 9 blast exposure significantly decreased R_{max} (**A**) in DG. Level 9 blast exposure significantly increased I_{50} (**B**) in CA3. Level 9 and Level 4 blast exposure levels reduced the parameter m (**C**) for all ROI; however, no change reached significance ($p > 0.09$ with a calculated power <0.56). Level 9 blast exposure significantly reduced PC1 (**D**) in DG. Mean ± SEM; $n \geq 5$, $^*p < 0.05$, as compared with sham. SEM, standard error of mean.

mechanical TBI were similar to the complex *in vivo* results. Cell-death-inducing stretch injury (10% strain, $20\,s^{-1}$ rate) decreased fEPSP and population spike R_{max} in the hippocampus at 4 days post-injury.[55] Hippocampal R_{max} peaked as strain rate increased at high strain 4 to 6 days post-stretch injury, but reached a minimum as strain rate increased at low strain.[27] The same study also observed that I_{50} was increased after injury.[27] Although conflicting, previous investigations have demonstrated that normal neuronal transmission can be affected by injury, which our study confirms. The minimal changes we observed at lower impulse blast exposures (i.e., Level 2 and Level 4) suggests that normal neuronal transmission is less sensitive to primary blast exposure than LTP and GSI.

PPF is one form of short-term synaptic plasticity,[61] governed at different ISI (40–2000 ms) by presynaptic neurotransmitter release[62,63] along with $GABA_A$, $GABA_B$, and NMDA receptor dynamics.[32–36] In our study, primary blast exposure did not affect PPR. The lack of changes in short-term plasticity observed in this study suggests that damage to presynaptic cellular machinery may not be responsible for the LTP deficits we observed.[46,64] Previous FPI studies have shown reduced paired-pulse inhibition (PPI) at short-term (<100 ms) ISIs and at mid-length (~500 ms) ISIs in rat CA1.[65] PPI was similarly reduced in rat hippocampal slices after mild stretch *in vitro* at shorter ISIs (<100 ms) in response to MF stimulation; however, PPI increased when exposed to low strain, high-strain rates at late-mid length ISIs (~500 ms), in response to SC stimulation.[27] In these time windows, paired-pulse depression is driven by $GABA_A$ and $GABA_B$ receptors, respectively.[32,33] The lack of effect of blast on PPR in our study suggests that GABA-mediated depression was not appreciably altered, but would require further testing to confirm. The difference in outcomes at the short-term and late-mid ISIs may be related to differences between the injury-models employed in each study, suggesting that changes in PPF may not be a blast-related phenomenon.

The blast levels tested in our study are similar to those commonly experienced in-theater.[3] Our Level 1 exposure is similar to the blast from an M49A4 60-mm mortar round at a standoff distance of 0.25–2 m, and the Level 9 exposure represents an explosion from an M118 bomb at a standoff distance of 10–32 m, according to the Conventional Weapons Effect Program (ConWEP). Our experimental conditions, whether unscaled or scaled for different species,[57] are consistent with the range of real-world blast exposures encountered by service members.

Although we report that primary blast exposure disrupted LTP and neuronal synchronization, there are limitations associated with this study. Translating the electrophysiological alterations measured *in vitro* to behavioral or cognitive changes *in vivo* is difficult[8,11,66]; however, our model provided the benefit of precise control over injury biomechanics, which remains a challenge for *in vivo* systems. Another limitation of this model is the inherent difficulty in translating tissue-level results to macroscopic loading scenarios. However, one of this study's strengths is the extensive characterization of pressure histories from the shock tube and the sample receiver. Measured fluid pressure histories applied to the tissue in the receiver could be extended to macroscopic loading conditions via realistic finite element models, which provide an intermediate step in the clinical understanding of tissue-level results. In the current study, neuronal activity was recorded at only one time frame (4–6 days) post-injury, which was chosen to allow for secondary injury cascades to develop but before regeneration mechanisms could repair damaged circuits.[3,19,22] One potentially important injury mechanism that is not reproduced with our *in vitro* model is the breakdown of the blood–brain barrier following blast exposure, which is increasingly a common observation in both *in vivo* and *in vitro* models.[67–72] Therefore, future studies will examine the time course of electrophysiological changes after blast. In our study, cell viability was a major outcome measure; however, other more subtle structural or protein alterations could be responsible for the observed electrophysiological deficits.

In summary, we report that primary blast disrupted LTP and decreased the synchronization of spontaneous activity in the hippocampus, while minimally affecting other functional measures. Disruption of LTP was dose-dependent with respect to blast impulse in the absence of cell death. Future studies will examine the molecular mechanisms underlying disruption of LTP.

Acknowledgments

This work was supported in part by a Multidisciplinary University Research Initiative from the Army Research Office (W911NF-10-1-0526) and by a National Defense Science and Engineering Graduate Fellowship from the Department of Defense (EWV-2012). The authors thank Jessica Villacorta for her skilled technical assistance with experimental setup and electrophysiological recording.

Author Disclosure Statement

No competing financial interests exist.

References

1. Huang, M., Risling, M., and Baker, D.G. (2015). The role of biomarkers and MEG-based imaging markers in the diagnosis of post-traumatic stress disorder and blast-induced mild traumatic brain injury. Psychoneuroendocrinology. [Epub ahead of print]
2. DVBIC (2015). Department of Defense Numbers for Traumatic Brain Injury. Armed Forces Health Surveillance Center: Defense and Veterans Brain Injury Center (DVBIC). http://dvbic.dcoe.mil/dod-worldwide-numbers-tbi
3. Effgen, G.B., Vogel III, E.W., Lynch, K.A., Lobel, A., Hue, C.D., Meaney, D.F., Bass, C.R., and Morrison III, B. (2014). Isolated primary blast alters neuronal function with minimal cell death in organotypic hippocampal slice cultures. J. Neurotrauma 31, 1202–1210.
4. Keyes, D.C. (2005). *Medical Response to Terrorism: Preparedness and Clinical Practice*. Lippincott Williams & Wilkins, Philadelphia, PA.
5. Morrison, B., 3rd, Elkin, B.S., Dolle, J.P., and Yarmush, M.L. (2011). In vitro models of traumatic brain injury. Annu. Rev. Biomed. Eng. 13, 91–126.
6. McIntosh, T.K., Vink, R., Noble, L., Yamakami, I., Fernyak, S., Soares, H., and Faden, A.L. (1989). Traumatic brain injury in the rat: characterization of a lateral fluid-percusssion model. Neuroscience 28, 233–244.
7. Cernak, I., Merkle, A.C., Koliatsos, V.E., Bilik, J.M., Luong, Q.T., Mahota, T.M., Xu, L., Slack, N., Windle, D., and Ahmed, F.A. (2011). The pathobiology of blast injuries and blast-induced neurotrauma as identified using a new experimental model of injury in mice. Neurobiol. Dis. 41, 538–551.
8. Patel, T.P., Gullotti, D.M., Hernandez, P., O'Brien, W.T., Capeheart, B.P., Morrison III, B., Bass, C.R., Eberwine, J.H., Abel, T., and Meaney, D.F. (2014). An open-source toolbox for automated phenotyping of mice in behavioral tasks. Front. Behav. Neurosci. 8, 1–16.
9. Wang, Y., Wei., Y., Oguntayo, S., Wilkins, W., Arun, P., Valiyaveettil, M., Song, J., Long, J.B., and Nambiar, M.P. (2011). Tightly coupled repetitive blast-induced traumatic brain injury: development and characterization in mice. J. Neurotrauma 28, 2171–2183.
10. Vandevord, P.J., Bolander, R., Sajja, V.S.S.S., Hay, K., and Bir, C.A. (2012). Mild neurotrauma indicates a range-specific pressure response to low level shock wave exposure. Ann. Biomed. Eng. 40, 227–236.
11. Goldstein, L.E., Fisher, A.M., Tagge, C.A., Zhang, X.L., Velisek, L., Sullivan, J.A., Upreti, C., Kracht, J.M., Ericsson, M., Wojnarowicz, M.W., Goletiani, C.J., Maglakelidze, G.M., Casey, N., Moncaster, J.A., Minaeva, O., Moir, R.D., Nowinski, C.J., Stern, R.A., Cantu, R.C., Geiling, J., Blusztajn, J.K., Wolozin, B.L., Ikezu, T., Stein, T.D., Budson, A.E., Kowall, N.W., Chargin, D., Sharon, A., Saman, S., Hall, G.F., Moss, W.C., Cleveland, R.O., Tanzi, R.E., Stanton, P.K., and McKee, A.C. (2012). Chronic traumatic encephalopathy in blast-exposed military veterans and a blast neurotrauma mouse model. Sci. Transl. Med. 4, 134ra160.
12. Elder, G.A., Dorr, N.P., De Gasperi, R., Gama Sosa, M.A., Shaughness, M.C., Maudlin-Jeronimo, E., Hall, A.A., McCarron, R.M., and Ahlers, S.T. (2012). Blast exposure induces post-traumatic stress disorder-related traits in a rat model of mild traumatic brain injury. J. Neurotrauma 29, 2564–2575.
13. Saljo, A., Svensson, B., Mayorga, M., Hamberger, A., and Bolouri, H. (2009). Low-level blasts raise intracranial pressure and impair cognitive function in rats. J. Neurotrauma 26, 1345–1352.
14. Gullotti, D.M., Beamer, M., Panzer, M.B., Chia Chen, Y., Patel, T.P., Yu, A., Jaumard, N., Winkelstein, B., Bass, C.R., Morrison, B., and Meaney, D.F. (2014). Significant head accelerations can influence immediate neurological impairments in a murine model of blast-induced traumatic brain injury. J. Biomech. Eng. 136, 091004–091004.
15. Svetlov, S.I., Prima, V., Kirk, D.R., Gutierrez, H., Curley, K.C., Hayes, R.L., and Wang, K.K.W. (2010). Morphologic and biochemical characterization of brain injury in a model of controlled blast overpressure exposure. J. Trauma Acute Care Surg. 69, 795–804.
16. Panzer, M.B., Matthews, K.A., Yu, A.W., Morrison, B., 3rd, Meaney, D.F., and Bass, C.R. (2012). A multiscale approach to blast neurotrauma modeling: Part I: Development of novel test devices for in vivo and in vitro blast injury models. Front. Neurol. 3, 46.
17. Effgen, G.B., Hue, C.D., Vogel, E., 3rd, Panzer, M.B., Meaney, D.F., Bass, C.R., and Morrison, B., 3rd. (2012). A multiscale approach to blast neurotrauma modeling: Part II: Methodology for inducing blast injury to in vitro models. Front. Neurol. 3, 23.
18. Shepard, S.R., Ghajar, J.B.G., Giannuzzi, R., Kupferman, S., and Hariri, R.I. (1991). Fluid percussion barotrauma chamber: A new in vitro model for traumatic brain injury. J. Surg. Res. 51, 417–424.
19. Wallis, R.A., and K.L. Panizzon (1995). Felbamate neuroprotection against CA1 traumatic neuronal injury. European J. Pharma. 294, 475–482.
20. Morrison, B., 3rd, Cater, H.L., Benham, C.D., and Sundstrom, L.E. (2006). An in vitro model of traumatic brain injury utilising two-dimensional stretch of organotypic hippocampal slice cultures. J. Neurosci. Methods 150, 192–201.
21. Cater, H.L., Sundstrom, L.E., and Morrison, B., 3rd. (2006). Temporal development of hippocampal cell death is dependent on tissue strain but not strain rate. J. Biomech. 39, 2810–2818.
22. Yu, Z., and Morrison III, B. (2010). Experimental mild traumatic brain injury induces functional alteration of the developing hippocampus. J. Neurophysiol. 103, 499–510.
23. Choi, J.H., Jung, H.K., and Kim, T. (2006). A new action potential detector using the MTEO and its effects on spike sorting systems at low signal-to-noise ratios. IEEE Trans Biomed Eng 53, 738–746.
24. Patel, T.P., Man, K., Firestein, B.L., and Meaney, D.F. (2015). Automated quantification of neuronal networks and single-cell calcium dynamics using calcium imaging. J. Neurosci. Methods 243, 26–38.
25. Kang, W.H., and Morrison III, B. (2015). Predicting changes in cortical electrophysiological function after in vitro traumatic brain injury. Biomech. Model Mechanobiol., 1–12.
26. Kang, W.H., Cao, W., Graudejus, O., Patel, T.P., Wagner, S., Meaney, D.F., and Morrison III, B. (2015). Alterations in hippocampal network activity after *in vitro* traumatic brain injury. J. Neurotrauma 32, 1011–1019.
27. Kang, W.H., and Morrison III, B. (2014). Functional tolerance to mechanical deformation developed from organotypic hippocampal slice cultures. Biomech. Model Mechanobiol. 14, 561–575.
28. Li, X., Cui, D., Jiruska, P., Fox, J.E., Yao, X., and Jefferys, J.G. (2007). Synchronization measurement of multiple neuronal populations. J. Neurophysiol. 98, 3341–3348.
29. Li, X., Ouyang, G., Usami, A., Ikegaya, Y., and Sik, A. (2010). Scale-free topology of the CA3 hippocampal network: a novel method to analyze functional neuronal assemblies. Biophys. J. 98, 1733–1741.
30. Patel, T.P., Ventre, S.C. and Meaney, D.F. (2012). Dynamic changes in neural circuit topology following mild mechanical injury in vitro. Ann.Biomed.Eng.40, 23–36.
31. Fueta, Y., Kawano, H., Ono, T., Mita, T., Fukata, K., and Ohno, K. (1998). Regional differences in hippocampal excitability manifested by paired-pulse stimulation of genetically epileptic El mice. Brain Res. 779, 324–328.
32. Stanford, I.M., Wheal, H.V., and Chad, J.E. (1995). Bicuculline enhances the late GABAB receptor-mediated paired-pulse inhibition observed in rat hippocampal slices. Eur. J. Pharmacol. 277, 229–234.
33. Margineanu, D.G., and Wulfert, E. (2000). Differential paired-pulse effects of gabazine and bicuculline in rat hippocampal CA3 area. Brain Res. Bull. 51, 69–74.
34. Joy, R.M., and Albertson, T.E. (1993). NMDA receptors have a dominant role in population spike-paired pulse facilitation in the dentate gyrus of urethane-anesthetized rats. Brain Res. 604, 273–282.
35. DiScenna, P.G., and Teyler, T.J. (1994). Development of inhibitory and excitatory synaptic transmission in the rat dentate gyrus. Hippocampus 4, 569–576.
36. Commins, S., Gigg, J., Anderson, M., and O'Mara, S.M. (1998). Interaction between paired-pulse facilitation and long-term potentiation in the projection from hippocampal area CA1 to the subiculum. Neuroreport 9, 4109–4113.

37. Zucker, R.S. (1989). Short-term synaptic plasticity. Annu. Rev. Neurosci. 12, 13–31.
38. Hu, D., Cao, P., Thiels, E., Chu, C.T., Wu, G., Oury, T.D., and Klann, E. (2007). Hippocampal long-term potentiation, memory, and longevity in mice that overexpress mitochondrial superoxide dismutase. Neurobiology of Learning and Memory 87, 372–384.
39. Swant, J., and Wagner, J.J. (2006). Dopamine transporter blockade increases LTP in the CA1 region of the rat hippocampus via activation of the D3 dopamine receptor. Learn. Mem. 13, 161–167.
40. Heuschkel, M.O., Fejtl, M., Raggenbass, M., Bertrand, D., and Renaud, P. (2002). A three-dimensional multi-electrode array for multisite stimulation and recording in acute brain slices. J. Neurosci. Methods 114, 135–148.
41. Axmacher, N., Mormann, F., Fernández, G., Elger, C.E., and Fell, J. (2006). Memory formation by neuronal synchronization. Brain Res. Rev. 52, 170–182.
42. Lyeth, B.G., Jenkins, L.W., Hamm, R.J., Dixon, C.E., Phillips, L.L., Clifton, G.L., Young, H.F., and Hayes, R.L. (1990). Prolonged memory impairment in the absence of hippocampal cell death following traumatic brain injury in the rat. Brain Res. 526, 249–258.
43. Gurkoff, G.G., Giza, C.C., and Hovda, D.A. (2006). Lateral fluid percussion injury in the developing rat causes an acute, mild behavioral dysfunction in the absence of significant cell death. Brain Res. 1077, 24–36.
44. D'Ambrosio, R., Maris, D.O., Grady, M.S., Winn, H.R., and Janigro, D. (1998). Selective loss of hippocampal long-term potentiation, but not depression, following fluid percussion injury. Brain Res. 786, 64–79.
45. Zhang, B., Chen, X., Lin, Y., Tan, T., Yang, Z., Dayao, C., Liu, L., Jiang, R., and Zhang, J. (2011). Impairment of synaptic plasticity in hippocampus is exacerbated by methylprednisolone in a rat model of traumatic brain injury. Brain Res. 1382, 165–172.
46. Schwarzbach, E., Bonislawski, B.P., Xiong, G., and Cohen, A.S. (2006). Mechanisms underlying the ability to induce area CA1 LTP in the mouse after traumatic brain injury. Hippocampus 16, 541–550.
47. Sanders, M.J., Sick, T.J., Perez-Pinzon, M.A., Dietrich, W.D., and Green, E.J. (2000). Chronic failure in the maintenance of long-term potentiation following fluid-percussion injury in the rat. Brain Res. 861, 69–76.
48. Thibault, L.E., Meaney, D.F., Anderson, B.J., and Marmarou, A. (1992). Biomechanical aspects of a fluid percussion model of brain injury. J. Neurotrauma 9, 311–322.
49. Dixon, C.E., Lyeth, B.G., Povlishock, J.T., Findling, R.L., Hamm, R.J., Marmarou, A., Young, H.F., and Hayes, R.L. (1987). A fluid percussion model of experimental brain injury in the rat. J. Neurosurg. 67, 110–119.
50. Sponheim, S.R., McGuire, K.A., Kang, S.S., Davenport, N.D., Aviyente, S., Bernat, E.M., and Lim, K.O. (2011). Evidence of disrupted functional connectivity in the brain after combat-related blast injury. NeuroImage 54, 521–529.
51. Tsirka, V., Simos, P.G., Vakis, A., Kanatsouli, K., Vourkas, M., Erimaki, S., Pachou, E., Stam, C.J., and Micheloyannis, S. (2011). Mild traumatic brain injury: graph-model characterization of brain networks for episodic memory. Int. J. Psychophysiol. 79, 89–96.
52. Wang, X.J. (2001). Synaptic reverberation underlying mnemonic persistent activity. Trends Neurosci. 24, 455–463.
53. Compte, A. (2006). Computational and *in vitro* studies of persistent activity: edging towards cellular and synaptic mechanisms of working memory. Neuroscience 139, 135–151.
54. Griesemer, D., and Mautes, A.M. (2007). Closed head injury causes hyperexcitability in rat hippocampal CA1 but not in CA3 pyramidal cells. J. Neurotrauma 24, 1823–1832.
55. Cater, H.L., Gitterman, D.P., Davis, S.M., Benham, C.D., Morrison III, B., and Sundstrom, L.E. (2007). Stretch-induced injury in organotypic hippocampal slice cultures reproduces in vivo post-traumatic neurodegeneration: role of glutamate receptors and voltage-dependent calcium channels. J. Neurochemistry 101, 434–447.
56. Park, E., Gottlieb, J.J., Cheung, B., Shek, P.N., and Baker, A.J. (2011). A model of low-level primary blast brain trauma results in cytoskeletal proteolysis and chronic functional impairment in the absence of lung barotrauma. J. Neurotrauma 28, 343–357.
57. Panzer, M.B., Wood, G.W., and Bass, C.R. (2014). Scaling in neurotrauma: how do we apply animal experiments to people? Exp. Neurol. 261, 120–126.
58. Witgen, B.M., Lifshitz, J., Smith, M.L., Schwarzbach, E., Liang, S.-L., Grady, M.S., and Cohen, A.S. (2005). Regional hippocampal alteration associated with cognitive deficit following experimental traumatic brain injury: a systems, network, and cellular evaluation. Neuroscience 133, 1–15.
59. Tran, L.D., Lifshitz, J., Witgen, B.M., Schwarzbach, E., Cohen, A.S., and Grady, M.S. (2006). Response of the contralateral hippocampus to lateral fluid percussion brain injury. J. Neurotrauma 23, 1330–1342.
60. Akasu, T., Muraoka, N., and Hasuo, H. (2002). Hyperexcitability of hippocampal CA1 neurons after fluid percussion injury of the rat cerebral cortex. Neurosci. Lett. 329, 305–308.
61. Salin, P.A., Scanziani, M., Malenka, R.C., and Nicoll, R.A. (1996). Distinct short-term plasticity at two excitatory synapses in the hippocampus. Proc. Natl. Acad. Sci. U S A 93, 13304–13309.
62. Schulz, P.E., Cook, E.P., and Johnston, D. (1994). Changes in paired-pulse facilitation suggests presynaptic involvement in long-term potentiation. Neuroscience 14, 5325–5337.
63. Wu, L.G., and Saggau, P. (1994). Presynaptic calcium is increased during normal synaptic transmission and paired-pulse facilitation, but not in long-term potentiation in area CA1 of hippocampus. Neuroscience 14, 645–654.
64. Schulz, P.E., Cook, E.P., and Johnston, D. (1995). Using paired-pulse facilitation to probe the mechanisms for long-term potentiation (LTP). J. Physiol. 89, 3–9.
65. Reeves, T.M., Lyeth, B.G., Phillips, L.L., Hamm, R.J., and Povlishock, J.T. (1997). The effect of traumatic brain injury on inhibition in the hippocampus and dentate gyrus. Brain Res. 757, 119–132.
66. Yin, T.C., Britt, J.K., Ready, J.M., and Pieper, A.A. (2014). P7C3 neuroprotective chemicals block axonal degeneration and preserve function after traumatic brain injury. Cell Rep. 8, 1731–1740.
67. Hue, C.D., Cao, S., Haider, S.F., Vo, K.V., Effgen, G.B., Vogel III, E.W., Panzer, M.B., Bass, C.R., Meaney, D.F., and Morrison III, B. (2013). Blood-brain barrier dysfunction after primary blast injury in vitro. J. Neurotrauma 30, 1652–1663.
68. Abdul-Muneer, P.M., Schuetz, H., Wang, F., Skotak, M., Jones, J., Gorantla, S., Zimmerman, M.C., Chandra, N., and Haorah, J. (2013). Induction of oxidative and nitrosative damage leads to cerebrovascular inflammation in an animal model of mild traumatic brain injury induced by primary blast. Free Radic. Biol. Med. 60, 282–291.
69. Yeoh, S., Bell, E.D., and Monson, K.L. (2013). Distribution of blood–brain barrier disruption in primary blast injury. Ann. Biomed. Eng. 41, 2206–2214.
70. Garman, R.H., Jenkins, L.W., Switzer, R.C., Bauman, R.A., Tong, L.C., Swauger, P.V., Parks, S.A., Ritzel, D.V., Dixon, C.E., Clark, R.S.B., Bayır, H., Kagan, V., Jackson, E.K., and Kochanek, P.M. (2011). Blast exposure in rats with body shielding is characterized primarily by diffuse axonal injury. J. Neurotrauma 28, 947–959.
71. Readnower, R.D., Chavko, M., Adeeb, S., Conroy, M.D., Pauly, J.R., McCarron, R.M., and Sullivan P.G. (2010). Increase in blood–brain barrier permeability, oxidative stress, and activated microglia in a rat model of blast-induced traumatic brain injury. J. Neurosci. Res. 88, 3530–3539.
72. Hue, C.D., Cao, S., Bass, C.R., Meaney, D.F., and Morrison III, B. (2014). Repeated primary blast injury causes delayed recovery, but not additive disruption, in an in vitro blood-brain barrier model. J. Neurotrauma 31, 951–960.

Address Correspondence to:
Barclay Morrison III, PhD
Columbia University
Department of Biomedical Engineering
1210 Amsterdam Avenue
New York, NY 10027

E-mail: bm2119@columbia.edu